Metric for three-dimensional alignment of molecules

Varun Makhija, Xiaoming Ren, and Vinod Kumarappan*

James R. Macdonald Laboratory, Department of Physics, Kansas State University, Manhattan, Kansas 66506, USA

(Received 12 November 2011; published 29 March 2012)

In an effort to clarify the three-dimensional alignment dynamics of polyatomic molecules, we propose a single measure for the degree of angular confinement of such molecules. The measure proposed for three-dimensional orientation is the angle of the single rotation that takes the molecule to the desired target orientation. Further, taking into account the D_2 symmetry of a three-dimensionally aligned distribution, a symmetrized version of the measure is constructed that serves as a direct indicator of the degree of three-dimensional alignment of a distribution. The calculation of the rotational dynamics of iodobenzene under the influence of two cross-polarized laser pulses demonstrates the effectiveness of the proposed metric.

DOI: 10.1103/PhysRevA.85.033425 PACS number(s): 37.10.Vz, 42.50.Hz, 33.15.Bh, 33.80.−b

I. INTRODUCTION

Laser-induced molecular alignment has become an important tool in molecular physics over the past decade. The interaction of a molecule's nonresonant polarizability with an intense laser pulse can be used to either hold it adiabatically or to set up a coherent rotational wave packet that aligns when the laser pulse is over [1]. Since the interaction is nonresonant, a variety of molecules can be aligned with the same laser, typically a Nd:YAG or Ti:sapphire laser, and the strong-field interaction ensures that all molecules in the laser focus are aligned. The experiments made possible by this technique include high-harmonic generation from aligned molecules [2], laser-induced electron diffraction [3], molecular frame photoelectron angular distribution measurements [4–6] even from molecules that do not fragment when ionized, control of filamentation of intense laser pulses in air [7], and ultrafast optical phase modulation [8]. Most of these applications have used linear molecules for which only one-dimensional (1D) alignment of the molecular axis is required. For asymmetric top molecules, it is necessary to align the molecules along all three axes in the laboratory frame (LF) in order to make measurements in the molecular frame (MF). In fact, depending on the number of mirror planes the molecule has, orientation of one or more axes will be required if the goal of molecular frame measurements is to be attained. Several experiments have shown three-dimensional (3D) alignment [9,10] and even 1D orientation combined with 3D alignment for molecules with two mirror planes [11,12]. Full 3D orientation has been discussed theoretically [13] but, to the best of our knowledge, has not yet been demonstrated.

For linear molecules, the characterization of alignment and orientation is based on a straightforward metric—the cosine of the angle between the desired alignment axis and the axis of the molecule. Quantifying alignment and orientation is somewhat more complex in three dimensions. Broadly speaking, two approaches have been adopted—using Euler angles [14] and direction cosines [15–17]—but neither is very satisfactory. Here we propose the adoption of a unifying scheme for quantifying the degree of alignment or orientation of molecules. Euler's rotation theorem guarantees that a single rotation can take an arbitrarily oriented rigid body to a target orientation, and we will show that the angle of this rotation can be used to characterize the degree of alignment and orientation of molecules.

Expectation values of $\cos^2\alpha$, where α is one of the three Euler angles θ, ϕ, and χ, are used for characterizing 3D alignment in Refs. [14,18]. (We will follow the convention used by Zare [19], in which *XYZ* is the LF coordinate system, *xyz* is the MF coordinate system, and θ, ϕ, and χ are the Euler angles.) The Euler angles have the advantage that they are independent variables and are used very widely to describe the physics of rigid body motion, but alignment in 3D requires the creation of distributions in which these angles are correlated. For example, we will show that only the sum and difference of the angles ϕ and χ, and not the angles themselves, matter for 3D alignment. For this reason the $\langle\cos^2\alpha\rangle$ are not ideal for characterizing 3D alignment.

The direction cosines ($\hat{x}\cdot\hat{X}=\cos\theta_{xX}, \hat{y}\cdot\hat{X}=\cos\theta_{yX}$, etc.) were used in Refs. [15,16]. But the direction cosines measure the alignment of individual molecular axes with their target locations instead of measuring the alignment of the MF with LF. Thus, quantifying 3D alignment requires not only $\langle\cos^2\theta_{ii}\rangle$ (we will use θ_{ij} as a collective symbol for the angles between the MF and LF coordinate axes) but some other $\langle\cos^2\theta_{ij}\rangle$'s, too. Any conclusions about 3D alignment require careful examination of the temporal evolution of all these variables.

In both cases, at least three 1D plots are required for characterizing 3D alignment. These plots are not easy to interpret, especially when the degree of alignment is not very strong. They also leave open to qualitative interpretation the comparison of 3D alignment in different types of experiments. For instance, is it better to have one angle strongly confined and the others not so well confined, or to equally confine all of them? In particular, how should an optimization algorithm score the two cases? Both the Euler angles and the direction cosines approaches suffer from these shortcomings. In this paper, we will show that using the axis-angle representation provides a unifying framework for all alignment and orientation experiments and addresses these issues in an adequate manner. The angle of rotation in this representation is a metric on the rotation group SO(3), and we will show that its cosine serves as the basis for defining a single measure for 3D alignment that reflects the symmetries

*vinod@phys.ksu.edu

of 3D-aligned ensembles of molecules. In Sec. II we introduce our measure for 3D alignment and derive the expressions required to calculate it. In Sec. III we demonstrate the efficacy of the measure by showing results of a calculation of the 3D alignment of iodobenzene, a near-prolate asymmetric top. We summarize our results and briefly discuss how such a measure can be useful in experiments in Sec. IV.

II. A SINGLE MEASURE FOR 3D ALIGNMENT

The problem of specifying a metric for 1D alignment of linear molecules is particularly simple. The space of possible orientations is the surface of a unit sphere. Since we are interested in the displacement of the members of the molecular ensemble from a laboratory-fixed axis, it is very convenient to chose this axis as the Z axis, and then measure the geodesic distance to each ensemble member on the unit sphere. This geodesic distance is quite intuitive—the cosine of the polar angle θ gives the length of the great circle arc that takes the z axis to the Z axis. The expectation value of $\cos\theta$ is widely accepted as a metric for characterizing 1D orientation of molecules. With this choice, a value of 1 denotes perfect orientation, and -1 denotes perfect antiorientation. When the Hamiltonian has a mirror plane perpendicular to the desired alignment axis—either due to a mirror plane perpendicular to the molecular axis or due to a symmetric field—every molecule at θ has an equivalent companion at $\pi - \theta$ and we use $\langle\cos^2\theta\rangle$ instead of the identically zero $\langle\cos\theta\rangle$. In this case, perfectly aligned, perfectly antialigned, and isotropic distributions have $\langle\cos^2\theta\rangle = 1, 0$, and $1/3$, respectively.

Our goal is to specify a similar scheme for 3D alignment. We show here that the use of the axis-angle representation of rotations in 3D is better suited for this purpose than either the Euler angle or the direction cosine representation. In this representation, arbitrary rotations are specified in terms of an angle and the unit vector along the axis of rotation. The angle δ_{if} of the rotation that takes initial orientation (θ_i,ϕ_i,χ_i) to the final orientation (θ_f,ϕ_f,χ_f) is a metric on SO(3), and the rotation is the geodesic path between the two orientations (for a discussion of this and other metrics on SO(3), see Ref. [20] and references therein). In terms of the rotation matrices $\mathbf{R}(\theta,\phi,\chi)$,

$$\cos\delta_{if} = \tfrac{1}{2}\{\mathrm{tr}[\mathbf{R}^T(\theta_i,\phi_i,\chi_i)\mathbf{R}(\theta_f,\phi_f,\chi_f)] - 1\}. \quad (1)$$

This metric does not depend on the choice of the coordinate system in which the Euler angles are defined—the trace is invariant when the coordinate system is rotated. The angle δ_{if} $(0 \leqslant \delta_{if} \leqslant \pi)$ is in radians. This angle is, thus, a natural choice for characterizing the degree of three-dimensional orientation of rigid molecules. The MF is the initial orientation and the LF is the final one [$\mathbf{R}(\theta_f,\phi_f,\chi_f)$ is the identity matrix in this case].

Although different vectors in the MF will be rotated by different angles when the MF is rotated by δ to make it coincide with the LF, no MF vector is displaced by an angle greater than δ. Therefore, δ is both the angle of a single rotation to the target and the worst possible separation of all MF axes from the corresponding LF axes. Thus, besides characterizing the distance between the MF and the LF in SO(3), the angle δ also provides information about the distribution of the individual MF axes. Due to these properties, $\langle\cos\delta\rangle$ is a good choice for a measure of 3D orientation. The values of $\langle\cos\delta\rangle$ for perfect orientation, perfect antiorientation, and for an isotropic distribution are $1, -1$, and $-1/2$, respectively. Note that unlike the 1D case, where $\theta = \pi$ is the only perfectly antioriented orientation, in 3D, there are infinitely many orientations that are perfectly antioriented since rotating a perfectly oriented molecule by π around *any* axis makes $\cos\delta = -1$.

In terms of the Euler angles, the direction cosines and the Wigner matrix elements, we have

$$\cos\delta = (\cos\theta + 1)[\cos(\phi + \chi) + 1]/2 - 1 \quad (2a)$$
$$= [\cos\theta_{xX} + \cos\theta_{yY} + \cos\theta_{zZ} - 1]/2 \quad (2b)$$
$$= \left[D^1_{11}(\mathbf{\Omega}) + D^1_{00}(\mathbf{\Omega}) + D^1_{-1-1}(\mathbf{\Omega}) - 1\right]/2. \quad (2c)$$

The last form, where $\mathbf{\Omega}$ is a collective symbol for the three Euler angles, is particularly useful for computation in the symmetric top basis, widely used for solving the Schrödinger equation for rigid-rotor dynamics.

Similar to 1D alignment, for 3D alignment we ignore the distinction between positive and negative directions for all the LF and MF axes. Since molecules are assumed to be rigid and have fixed handedness, there are four equivalent target orientations connected by a rotation of the LF along any of its Cartesian axes by π. These are shown in Fig. 1. The importance of considering these operations, which form the symmetry group D_2, in solving the Schödinger equation for the rotational dynamics of asymmetric tops has been highlighted by Pabst *et al.* [17]. We show here that the correct incorporation of the symmetry into the choice of observable allows the use of a single measure for 3D alignment. For every possible orientation of the MF, specified by the Euler angles θ, χ, and ϕ, we define four angles δ_F $(F = O,X,Y,Z)$, denoting the angles of the rotations that take the MF to the four target orientations. Here the subscript O denotes the LF and X, Y, and Z denote the target orientations generated by a π rotation around the corresponding LF axis. The rotation matrices describing the four target orientations themselves are diagonal, with elements $(1,1,1)$, $(1,-1,-1)$, $(-1,1,-1)$, and $(-1,-1,1)$ along the diagonal. Expressions for $\cos\delta_F$ are readily obtained by using

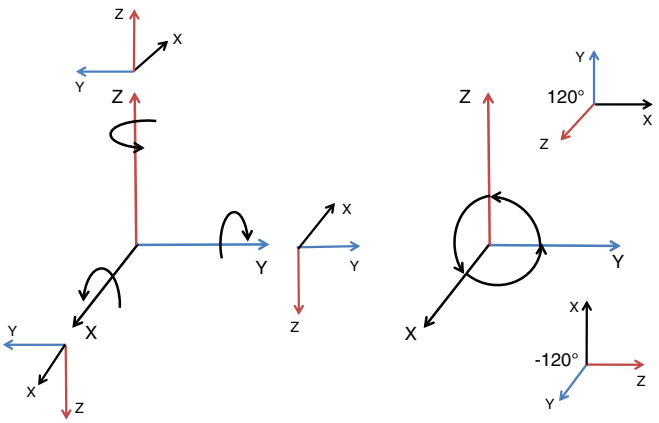

FIG. 1. (Color online) On the left, four equivalent target orientations for 3D alignment generated by π rotations around the LF axes. On the right, two of eight possible perfectly antialigned orientations in 3D. The axis of rotation is the unit vector $(\hat{X} + \hat{Y} + \hat{Z})/\sqrt{3}$. The remaining six can be generated from these two by π rotations around the X, Y, and Z axes.

Eqs. (1) and (2). In terms of the Euler angles,

$$\cos\delta_O = (1+\cos\theta)[1+\cos(\phi+\chi)]/2 - 1, \quad (3a)$$
$$\cos\delta_X = (1-\cos\theta)[1-\cos(\phi-\chi)]/2 - 1, \quad (3b)$$
$$\cos\delta_Y = (1-\cos\theta)[1+\cos(\phi-\chi)]/2 - 1, \quad (3c)$$
$$\cos\delta_Z = (1+\cos\theta)[1-\cos(\phi+\chi)]/2 - 1. \quad (3d)$$

These equations can be recast in terms of the Euler parameters: $\cos\delta_F = 2e_F^2 - 1$ [21]. These parameters generate a representation of rotations in terms of SU(2) matrices, and satisfy the constraint that $\sum_F e_F^2 = 1$, which ensures that rotations preserve the norms of vectors. In terms of the $\cos\delta_F$, this constraint becomes

$$\cos\delta_O + \cos\delta_X + \cos\delta_Y + \cos\delta_Z = -2. \quad (4)$$

This implies that the expectation value of each $\cos\delta_F$ for an isotropic distribution is $-1/2$—on average, the angle required to rotate a molecule to any one of the target orientations is 120°. In fact, for any distribution with D_2 symmetry $\langle\cos\delta_F\rangle$ must all be $-1/2$. Therefore, none of these cosines is suitable as a measure of 3D alignment. Further, for a given molecular orientation the $\cos^2\delta_F$ do not have the same value for each of the equivalent target orientations, making them unsuitable measures as well. We define instead the average of the $\cos^2\delta_F$,

$$\cos^2\delta \equiv \frac{1}{4}\sum_F \cos^2\delta_F, \quad (5)$$

as our measure for 3D alignment. The expectation values of the $\cos^2\delta_F$ must, of course, be the same for any D_2-symmetric distribution of molecules; if this is the case, the averaging is redundant. In terms of the direction cosines, it is easily seen that

$$\cos^2\delta = \tfrac{1}{4}(1+\cos^2\theta_{xX}+\cos^2\theta_{yY}+\cos^2\theta_{zZ}). \quad (6)$$

In this form, several properties of $\langle\cos^2\delta\rangle$ are apparent. For perfect alignment $\cos^2\delta = 1$. The expectation value for a uniform distribution of molecules is 1/2, while the minimum possible value is 1/4. The minimum is obtained for the worst 3D-aligned molecules, when each axis is perfectly antialigned and $\cos\delta_F$ are all $-1/2$. There are eight perfectly antialigned orientations—at $\theta = \pi/2$, $\phi = 0$ or π, and $\chi = \pm\pi/2$; and at $\theta = \pi/2$, $\chi = 0$ or π and $\phi = \pm\pi/2$—and a 120° rotation is required to bring them into alignment with any of the four target orientations. Two of these are shown in Fig. 1.

The matrix elements of $\cos^2\delta$ in the symmetric top basis ($|JKM\rangle$, where J is the total angular momentum and K and M are the projections along the z axis and the Z axis, respectively) are

$$\langle JKM|\cos^2\delta|J'K'M'\rangle = \frac{1}{4} + \left[\frac{1}{4}\delta_{JJ'}\delta_{KK'}\delta_{MM'} + \frac{1}{4}\sqrt{\frac{2J+1}{2J'+1}}\langle J,M;2,0|J',M'\rangle\langle J,K;2,0|J',K'\rangle\right]$$
$$+\left[\frac{1}{8}\sqrt{\frac{2J+1}{2J'+1}}[\langle J,K;2,2|J',K'\rangle + \langle J,K;2,-2|J',K'\rangle][\langle J,M;2,2|J',M'\rangle\right.$$
$$\left.+\langle J,M;2,-2|J',M'\rangle]\right]. \quad (7)$$

Each matrix element splits into three terms. The constant 1/4 is the minimum value of $\cos^2\delta$, reflecting the fact that no MF is more than 120° away from perfect 3D alignment. The second term reflects the alignment of the z axis with the Z axis, and is directly related to the matrix element for $\cos^2\theta_{zZ}$ [Eq. (A1)]. The coherences that contribute to this term involve $\Delta J = 0,\pm1,\pm2$ and $\Delta K, M = 0$. The last term contains the contributions of coherences that involve $\Delta K = \pm2$ *and* $\Delta M = \pm2$ and thus the simultaneous motion of the molecules about the z and Z axes. There is no contribution from coherences in which $\Delta K = \pm2$ *or* $\Delta M = \pm2$. These coherences contribute to $\langle\cos^2\theta_{xX}\rangle$ [Eq. (A3)] and $\langle\cos^2\theta_{yY}\rangle$ [Eq. (A2)] but cancel out in $\langle\cos^2\delta\rangle$. This elucidates an essential feature of 3D alignment: Only *coupled motion* about the z and Z axes can contribute to 3D alignment. The absence of the third term, and the corresponding uncoupled motion can be traced back to the D_2 symmetry of 3D-aligned ensembles. The value of one of the $\cos\delta_F$ (and hence 3D orientation) can be improved by uncoupled rotation of a molecule about either the z or the Z axes, but D_2 symmetry introduces the three additional target orientations shown in Fig. 1. Bringing molecules to each of these orientations simultaneously necessitates coupled motion about the z and Z axes. This feature is evident in Eq. (3), where the Euler angles χ and ϕ—variables conjugate to K and M, respectively—appear only in pairs.

Alignment schemes that use two cross-polarized pulses [10,22] rely on changing both quantum numbers simultaneously by first getting the z and Z axes as close to each other as possible. In the limit of perfect 1D alignment of the z axis, χ and ϕ become degenerate and the motion is necessarily coupled.

If the z axis is perfectly aligned with the Z axis, the x and y axes are necessarily confined to the XY plane. If these axes are uniformly distributed in the XY plane, $\langle\cos^2\theta_{xX}\rangle = \langle\cos^2\theta_{yY}\rangle = 1/2$. In this case $\langle\cos^2\delta\rangle = 3/4$. Thus, the difference between 1D and 3D alignment is just a matter of degree—aligning only in one dimension brings the distribution closer to the target distribution in 3D and should be considered a limited form of 3D alignment. We would like to note here that the seemingly special status of 1D alignment of the z axis along the Z axis is the result of the choice of the symmetric top basis—perfect 1D alignment of *any* MF axis with the corresponding LF axis will make $\langle\cos^2\delta\rangle = 3/4$. In fact, the invariance of $\cos\delta_{if}$ [Eq. (1)] under rotations of the coordinate system implies that the target orientations need not coincide with the

LF at all: The 3D measure defined in Eq. (5) inherits the invariance.

III. THREE-DIMENSIONAL ALIGNMENT OF IODOBENZENE

In order to clarify the dynamics of 3D alignment in terms of $\cos^2\delta$, we solve the time-dependent Schrödinger equation (TDSE) for an asymmetric top molecule in an intense laser field interacting through the nonresonant polarizability tensor [14,17]. Iodobenzene is used as an example. We assume that the laser pulse excites only rotational Raman transitions from the initial ground vibronic state, and centrifugal distortion is not taken into account. A thermal distribution of initial asymmetric top states, including the nuclear spin statistics of iodobenzene [23], is used. No averaging over the laser focal volume is carried out; the results shown are for a single laser intensity.

The time-dependent Hamiltonian is

$$H = H_{\rm rot} - \tfrac{1}{4}\mathbf{E}(t)\cdot[\boldsymbol{\alpha}\mathbf{E}(t)], \tag{8}$$

where $H_{\rm rot} = AJ_a^2 + BJ_b^2 + CJ_c^2$ is the field-free Hamiltonian for an asymmetric rigid rotor, $\boldsymbol{\alpha}$ is the polarizability tensor of the molecule, and $\mathbf{E}(t)$ is the laser electric field. The electric field for linearly or elliptically polarized laser pulses is

$$\mathbf{E}(t) = E_0(t)[\epsilon_X\cos(\omega t)\mathbf{e}_X + \epsilon_Z\sin(\omega t)\mathbf{e}_Z], \tag{9}$$

where ω is the field frequency and $E_0(t)$ is the time-dependent field envelope that is assumed to be Gaussian. $\mathbf{e}_X$ and $\mathbf{e}_Z$ represent unit vectors in the X and Z directions. The z axis in the MF is chosen to be along the C-I bond, and the y axis is perpendicular to the plane of the ring. The field polarization is determined by ϵ_X and ϵ_Z, which are constrained by $\epsilon_X^2 + \epsilon_Z^2 = 1$. The symmetric top basis is used to the solve the TDSE in the laser field by using an adaptive step-size Dormand-Prince method [24], and the field-free wave packet is propagated in the asymmetric top basis.

The results of TDSE calculations for iodobenzene, a near-prolate top, subject to a single linearly polarized pulse and to two time-separated, orthogonally polarized pulses are shown in Fig. 2. The one-pulse trace in Fig. 2(c) shows the expected behavior of $\langle\cos^2\theta_{zZ}\rangle$ after excitation by a single linearly polarized pulse. J- and C-type revivals, resulting from $\Delta J = \pm1,\pm2, \Delta K = 0$ and $\Delta J = \pm2, \Delta K = 0$ coherences [25], respectively, are seen in a pattern that has previously been observed [26]. The corresponding traces in Figs. 2(a) and 2(b) show the evolution of $\langle\cos^2\theta_{xX}\rangle$ and $\langle\cos^2\theta_{yY}\rangle$, respectively. Linearly polarized pulses do interact with the angle χ for asymmetric tops, and this results in the appearance of K-type revivals ($\Delta J = 0, \Delta K = \pm2$) in these two variables. From Fig. 3 it is clear that $\langle\cos^2\delta\rangle$ reflects the behavior of $\langle\cos^2\theta_{zZ}\rangle$, as expected from Eq. (7). According to the description suggested here, this should be viewed as 3D alignment in the sense that even 1D alignment moves the molecules closer to the target orientations for 3D alignment. The K-type coherences seen in $\langle\cos^2\theta_{xX}\rangle$ and $\langle\cos^2\theta_{yY}\rangle$ cancel out because they are out of phase and do not contribute to 3D alignment at all.

For two crossed-polarized pulses, however, we see that the behavior of $\langle\cos^2\delta\rangle$ (Fig. 3) does not reflect that of any

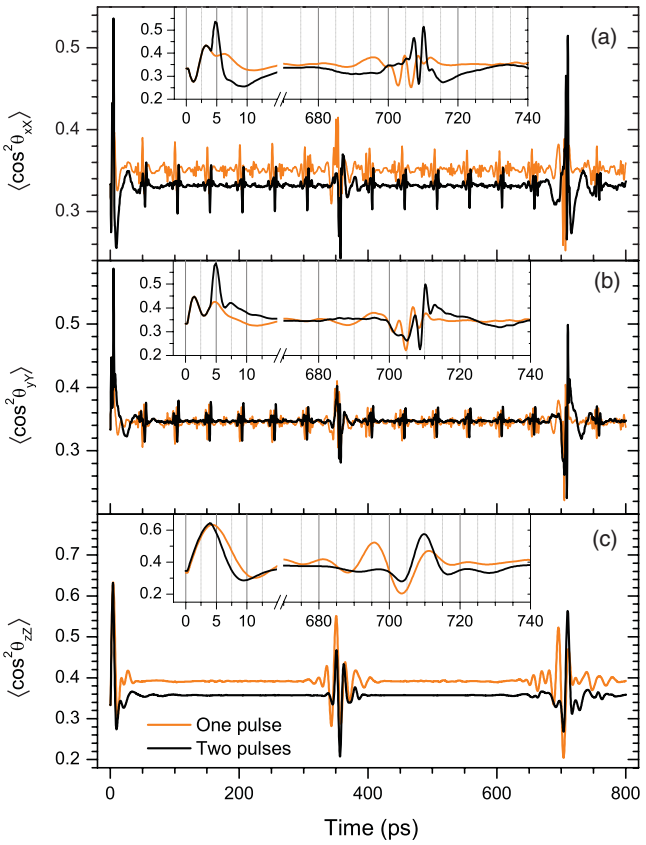

FIG. 2. (Color online) Expectation values calculated using TDSE for one-pulse and two-pulse excitation of rotational wave packets. The single pulse and the first pulse of the two-pulse calculation are polarized along the Z axis and peak at 0 ps; the second pulse is polarized along the X axis and peaks at 3.8 ps. Each pulse has a Gaussian temporal envelope with a duration (full width at half maximum of the intensity) of 170 fs and a peak intensity of 8 TW/cm^2. The rotational temperature of iodobenzene is 0.5 K. The insets show details of the initial alignment and the second J-type revival.

individual direction cosine. After the second pulse $\langle\cos^2\theta_{xX}\rangle$ and $\langle\cos^2\theta_{yY}\rangle$ (Fig. 2) rise sharply, indicating that the MF x and y axes are being driven to the LF X and Y axes. $\langle\cos^2\theta_{zZ}\rangle$, however, begins to drop after the second pulse, indicating that the molecular z axis is being driven away from the laboratory Z axis. In this case, since the z axis of iodobenzene rotates much slower than the other two axes, it has not strayed very far when the other axes reach their peak alignment (at about 4.8 ps), thus producing a 3D-aligned population. The crucial idea is that this information is available from $\langle\cos^2\delta\rangle$ alone. We see that after the second pulse $\langle\cos^2\delta\rangle$ rises sharply and peaks at 4.73 ps, indicating that the second pulse drives the molecules further toward 3D alignment, and the best 3D alignment occurs at 4.73 ps.

In the two-pulse case $\langle\cos^2\delta\rangle$ (Fig. 3) has an interesting revival structure, too. Now the K-type revivals in $\langle\cos^2\theta_{xX}\rangle$ and $\langle\cos^2\theta_{yY}\rangle$ are no longer out of phase and do contribute to $\langle\cos^2\delta\rangle$ as well, indicating coupled rotation around the z and Z axes. These revivals in $\langle\cos^2\delta\rangle$ are not K-type revivals since the selections rules governing them are $\Delta K, M = \pm2$. But since the field-free energies of the rotational eigenstates do

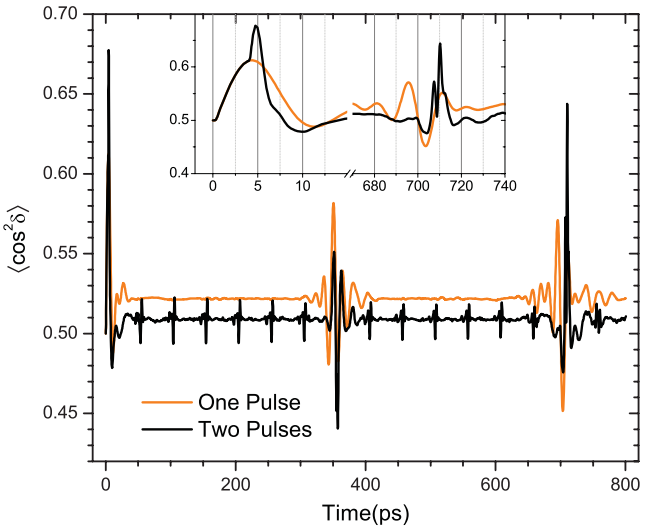

FIG. 3. (Color online) The expectation values of $\langle \cos^2 \delta \rangle$ for the excitation schemes shown in Fig. 2. The evolution of 3D alignment can be seen directly in this variable. Apart from the initial 3D alignment after the second pulse, the overlap of J- and K-type revivals results in a substantial revival of 3D alignment at 710.2 ps.

not depend on M, the periodicity of these revivals is the same as that of K-type revivals. Once again, the maxima exhibited at these revivals are also local maxima in 3D alignment, limited in the same sense that 3D alignment in the the single-pulse case was limited. Here it is the evolution of $\langle \cos^2 \theta_{zZ} \rangle$ that does not contribute to the revivals. Coincidentally, the 14th K-type revival overlaps with the second J-type revival, producing a sharp spike in $\langle \cos^2 \delta \rangle$ at 710.2 ps, representing a substantial revival of the initial 3D alignment. In general, 3D alignment revivals have to rely on such coincidences, where two different types of revivals together involve all three molecular axes and occur in close proximity to each other. Due to the finite temporal extent of the revivals, it is only necessary for the revival periods to be approximately commensurate for these overlaps to occur. In the manner of revivals in the 1D alignment of asymmetric tops, these 3D revivals will neither be complete nor truly periodic but might nevertheless be substantial.

IV. SUMMARY

We have proposed a unified method for quantifying the three-dimensional alignment of molecules using a single scalar quantity that handles the symmetries of the molecular axis distribution correctly. The proposed measure is based on a metric on the rotational group that also serves as a measure of 3D orientation and has several advantages over schemes used currently. First, the measure is easy to interpret physically—it gives the value of the *smallest* angle by which molecules need to be rotated to bring them to a desired orientation. At the same time, it also provides the *largest* possible angle by which *any individual axis* might be separated from its desired orientation. Second, unlike other measures used in the literature, our measure provides a single number that works over the entire space of possible orientations, including perfect antialignment in three dimensions. This aspect is essential in designing better schemes to confine the orientation of molecules. In particular, such a measure should be very useful in optimization schemes, both in computational efforts as well as in experiments.

Coincident fragment momentum spectroscopy provides the most detailed measurements of 3D alignment since the full 3D orientation of each molecule can be determined by measuring the momenta of two or more fragment ions in coincidence. It is possible to evaluate $\langle \cos \delta \rangle$ and $\langle \cos^2 \delta \rangle$ from this information by first constructing the expectation values of $\langle \cos \theta_{ij} \rangle$ and $\langle \cos^2 \theta_{ij} \rangle$ and then using Eqs. (2b) and (6), respectively. But such coincidence experiments are feasible only for small molecules such as sulfur dioxide, and even these are subject to the influence of the probe pulse which selectively ionizes molecules in some orientations more effectively than others [27]. In the absence of coincident imaging, 3D alignment can still be characterized by momentum imaging techniques such as velocity map imaging when the degree of alignment of one axis is very good. This approach was taken in Refs. [12,22], where one axis was confined very strongly using an adiabatic field, allowing direct measurement of the molecular plane without coincidence measurements. However, a quantitative determination of $\langle \cos^2 \delta \rangle$ is not possible in this scheme, even if the full 3D momentum distribution of the fragment ions is reconstructed tomographically [28], due to the lack of sufficient information about the distribution of all the axes. We expect that the development of direct and rapid measurement techniques for $\langle \cos \delta \rangle$ and $\langle \cos^2 \delta \rangle$ will advance our ability to align and orient polyatomic molecules substantially.

ACKNOWLEDGMENTS

V.K. would like to thank Brett Esry for lending a thoughtful ear. This work was supported by the Chemical Sciences, Geosciences, and Biosciences Division, Office of Basic Energy Sciences, Office of Science, US Department of Energy, and Kansas State University.

APPENDIX: MATRIX ELEMENTS OF $\cos^2 \theta_{ii}$

The matrix elements of $\langle \cos^2 \theta_{ij} \rangle$ in the symmetric top basis, with terms grouped into the three types discussed in Sec. II, are

$$\langle JKM| \cos^2 \theta_{zZ} |J'K'M'\rangle = \left[\frac{1}{3}\delta_{JJ'}\delta_{KK'}\delta_{MM'} + \frac{2}{3}\sqrt{\frac{2J+1}{2J'+1}}\langle J,M;2,0|J',M'\rangle\langle J,K;2,0|J',K'\rangle\right], \tag{A1}$$

$$\langle JKM| \cos^2 \theta_{yY} |J'K'M'\rangle = \left[\frac{1}{3}\delta_{JJ'}\delta_{KK'}\delta_{MM'} + \frac{1}{6}\sqrt{\frac{2J+1}{2J'+1}}\langle J,M;2,0|J',M'\rangle\langle J,K;2,0|J',K'\rangle\right]$$
$$+\left[\frac{1}{2\sqrt{6}}\sqrt{\frac{2J+1}{2J'+1}}\{\langle J,M;2,0|J',M'\rangle[\langle J,K;2,2|J',K'\rangle + \langle J,K;2,-2|J',K'\rangle]\right.$$

$$+\langle J,K;2,0|J',K'\rangle[\langle J,M;2,2|J',M'\rangle+\langle J,M;2,-2|J',M'\rangle]\}\Big]$$
$$+\Big[\frac{1}{4}\sqrt{\frac{2J+1}{2J'+1}}\{[\langle J,K;2,2|J',K'\rangle+\langle J,K;2,-2|J',K'\rangle]$$
$$\times[\langle J,M;2,2|J',M'\rangle+\langle J,M;2,-2|J',M'\rangle]\}\Big], \tag{A2}$$

$$\langle JKM|\cos^2\theta_{xX}|J'K'M'\rangle=\Big[\frac{1}{3}\delta_{JJ'}\delta_{KK'}\delta_{MM'}+\frac{1}{6}\sqrt{\frac{2J+1}{2J'+1}}\langle J,M;2,0|J',M'\rangle\langle J,K;2,0|J',K'\rangle\Big]$$
$$-\Big[\frac{1}{2\sqrt{6}}\sqrt{\frac{2J+1}{2J'+1}}\{\langle J,M;2,0|J',M'\rangle[\langle J,K;2,2|J',K'\rangle+\langle J,K;2,-2|J',K'\rangle]$$
$$+\langle J,K;2,0|J',K'\rangle[\langle J,M;2,2|J',M'\rangle+\langle J,M;2,-2|J',M'\rangle]\}\Big]$$
$$+\Big[\frac{1}{4}\sqrt{\frac{2J+1}{2J'+1}}\{[\langle J,K;2,2|J',K'\rangle+\langle J,K;2,-2|J',K'\rangle]$$
$$\times[\langle J,M;2,2|J',M'\rangle+\langle J,M;2,-2|J',M'\rangle]\}\Big]. \tag{A3}$$

[1] H. Stapelfeldt and T. Seideman, Rev. Mod. Phys. **75**, 543 (2003).
[2] R. Velotta, N. Hay, M. B. Mason, M. Castillejo, and J. P. Marangos, Phys. Rev. Lett. **87**, 183901 (2001).
[3] M. Meckel, D. Comtois, D. Zeidler, A. Staudte, D. Pavičić, H. C. Bandulet, H. Pépin, J. C. Kieffer, R. Dörner, D. M. Villeneuve, and P. B. Corkum, Science **320**, 1478 (2008).
[4] V. Kumarappan, L. Holmegaard, C. Martiny, C. B. Madsen, T. K. Kjeldsen, S. S. Viftrup, L. B. Madsen, and H. Stapelfeldt, Phys. Rev. Lett. **100**, 093006 (2008).
[5] C. Bisgaard, O. Clarkin, G. Wu, A. Lee, O. Geßner, C. Hayden, and A. Stolow, Science **323**, 1464 (2009).
[6] J. L. Hansen, H. Stapelfeldt, D. Dimitrovski, M. Abu-samha, C. P. J. Martiny, and L. B. Madsen, Phys. Rev. Lett. **106**, 073001 (2011).
[7] S. Varma, Y. H. Chen, and H. M. Milchberg, Phys. Rev. Lett. **101**, 205001 (2008).
[8] R. A. Bartels, T. C. Weinacht, N. Wagner, M. Baertschy, C. H. Greene, M. M. Murnane, and H. C. Kapteyn, Phys. Rev. Lett. **88**, 013903 (2001).
[9] J. J. Larsen, K. Hald, N. Bjerre, H. Stapelfeldt, and T. Seideman, Phys. Rev. Lett. **85**, 2470 (2000).
[10] K. F. Lee, D. M. Villeneuve, P. B. Corkum, A. Stolow, and J. G. Underwood, Phys. Rev. Lett. **97**, 173001 (2006).
[11] H. Tanji, S. Minemoto, and H. Sakai, Phys. Rev. A **72**, 063401 (2005).
[12] I. Nevo, L. Holmegaard, J. H. Nielsen, J. L. Hansen, H. Stapelfeldt, G. Filsinger, Frankand Meijer, and J. Kupper, Phys. Chem. Chem. Phys. **11**, 9912 (2009).
[13] N. Takemoto and K. Yamanouchi, Chem. Phys. Lett. **451**, 1 (2008).
[14] T. Seideman and M. Artamonov, J. Chem. Phys. **128**, 154313 (2008).
[15] J. G. Underwood, B. J. Sussman, and A. Stolow, Phys. Rev. Lett. **94**, 143002 (2005).
[16] A. Rouzée, S. Guérin, O. Faucher, and B. Lavorel, Phys. Rev. A **77**, 043412 (2008).
[17] S. Pabst, P. J. Ho, and R. Santra, Phys. Rev. A **81**, 043425 (2010).
[18] M. Artamonov and T. Seideman, Phys. Rev. A **82**, 023413 (2010).
[19] R. N. Zare, *Angular Momentum: Understanding Spatial Aspects in Chemistry and Physics* (Wiley-Interscience, New York, 1988).
[20] D. Q. Huynh, J. Math. Imaging Vision **35**, 155 (2009).
[21] H. Goldstein, *Classical Mechanics*, 2nd ed. (Addison-Wesley, Reading, MA, 1980).
[22] S. S. Viftrup, V. Kumarappan, S. Trippel, H. Stapelfeldt, E. Hamilton, and T. Seideman, Phys. Rev. Lett. **99**, 143602 (2007).
[23] J. Bulthuis, J. Möller, and H. J. Loesch, J. Phys. Chem. A **101**, 7684 (1997).
[24] J. Dormand and P. Prince, J. Comput. Appl. Math. **6**, 19 (1980).
[25] P. W. Joireman, L. L. Connell, S. M. Ohline, and P. M. Felker, J. Chem. Phys. **96**, 4118 (1992).
[26] L. Holmegaard, S. S. Viftrup, V. Kumarappan, C. Z. Bisgaard, H. Stapelfeldt, E. Hamilton, and T. Seideman, Phys. Rev. A **75**, 051403 (2007).
[27] F. Légaré, K. F. Lee, I. V. Litvinyuk, P. W. Dooley, S. S. Wesolowski, P. R. Bunker, P. Dombi, F. Krausz, A. D. Bandrauk, D. M. Villeneuve, and P. B. Corkum, Phys. Rev. A **71**, 013415 (2005).
[28] M. Wollenhaupt, M. Krug, J. Köhler, T. Bayer, C. Sarpe-Tudoran, and T. Baumert, Appl. Phys. B **95**, 647 (2009).